Shear Process and Frictional Characteristics in Down-end Milling

Young-Moon Lee[1,#] and Seung-Il Jang[2]

[1] School of Mechanical Engineering, Kyungpook National University, Taegu, South Korea
[2] Graduate School of Mechanical Engineering, Kyungpook National University, Taegu, South Korea

ABSTRACT

In end milling process, which is characterized by the use of a rotating tool, the undeformed chip thickness varies periodically with phase change of the tool. Although many efforts have concentrated on the study of end milling process, the analysis of shear and chip-tool friction behaviors has not been reported. Recently, a model has been proposed to simulate the shear and friction characteristics of an up-end milling process in terms of the equivalent oblique cutting. In the current study, the varying undeformed chip thickness and the cutting forces in a down-end milling process are replaced with the equivalent ones of oblique cutting. Then it is possible to simulate the shear and the chip-tool friction characteristics of a down-end milling process. The proposed model has been verified through two sets of cutting tests i.e., down-end milling and the equivalent oblique cutting tests. The experimental results show that the proposed model is suitable to analyze the shear and chip-tool frictional characteristics of down-end milling process. The specific cutting energy decreases with increase in equivalent undeformed chip thickness in a down-end milling process.

Key Words : Down-end milling, Equivalent oblique cutting, Helix angle, Inclination angle, Specific shear energy, Specific friction energy, Specific cutting energy

Nomenclature

ϕ = cutter rotation angle
β = helix angle
i = inclination angle
S_t = feed per tooth
r = radius of tool
a = radial depth of cut
b = axial depth of cut
h = undeformed chip thickness
F_x = vertical cutting force component
F_y = horizontal cutting force component
F_z = axial cutting force component

F_r = radial cutting force component
F_t = tangential cutting force component

1. Introduction

In a metal cutting process, a chip is produced due to concentrated shear processes that occur at very small intervals in an extremely limited region, i.e., the shear zone. The produced chip experiences severe frictional interaction with the tool rake face before being externally discharged. Therefore, the study of a cutting process is based on the analysis of shear process in the shear zone and frictional characteristics in the chip-tool contact region. A great deal of research on the shear and frictional characteristics have been studied, but mostly in continuous cutting.

Martellotti[1] established the geometric relationships between the tool path and the cutting variables in the

intermittent cutting process of milling. Tlusty and Macneil[2] presented a mechanistic model for the prediction of cutting forces in up-end milling by multiplying an undeformed chip area by specific cutting forces, and verified the validity of the model by comparing the computed cutting forces with the measured ones. Many researchers[3~5] have made efforts to gain fundamental understanding of intermittent cutting processes. However, no analysis of the shear and frictional characteristics in intermittent cutting has yet been attempted. Recently, Lee et. al.[6] proposed a model to simulate the shear and frictional characteristics in an up-end milling process.

In the present paper, the shear and frictional characteristics of a down-end milling process based on the equivalent oblique cutting system has been analyzed and experimentally verified.

2. Down-end milling process model

2.1 Undeformed chip thickness

Fig. 1 shows a three-dimensional model of a down-end milling process with a two-tooth cutter along with the geometrical relations between the tool and the workpiece.

The maximum undeformed chip thickness, h_{max}, is represented by Eq. (1).

$$h_{max} = r - \sqrt{(r-a)^2 + \left\{\sqrt{r^2 - (r-a)^2} - s_t\right\}^2} \quad (1)$$

where ϕ_1 is the rotation angle when h reaches its maximum, and ϕ_2 is the rotation angle when the cutting edge escapes from the workpiece. ϕ_1 and ϕ_2 can be expressed by Eqs. (2) and (3), respectively.

$$\phi_1 = \cos^{-1}\left(\frac{r-a}{r-h_{max}}\right) \quad (2)$$

$$\phi_2 = \cos^{-1}\left(1 - \frac{a}{r}\right) \quad (3)$$

2.2 Cutting forces

Fig. 2 shows a cutting force model of a down-end milling process. F_x, F_y, and F_z are the vertical, horizontal and axial cutting force components, respectively. Also, F_r and F_t are the radial and tangential cutting force components, respectively. Cutting forces must be

calculated for each tooth as a function of the cutter rotation angle. Total forces are obtained by summing the forces on the teeth engaged in the cutting process. The relationship of the forces can be expressed by Eq. (4).

$$\begin{bmatrix} dF_x \\ dF_y \\ dF_z \end{bmatrix} = \begin{bmatrix} \cos(\phi_2-\phi) & \sin(\phi_2-\phi) & 0 \\ -\sin(\phi_2-\phi) & \cos(\phi_2-\phi) & 0 \\ 0 & 0 & 1 \end{bmatrix} \begin{bmatrix} dF_r \\ dF_t \\ dF_z \end{bmatrix} \quad (4)$$
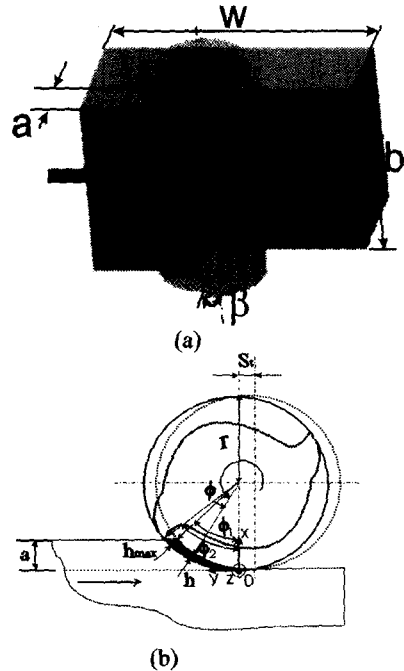

(a)

(b)

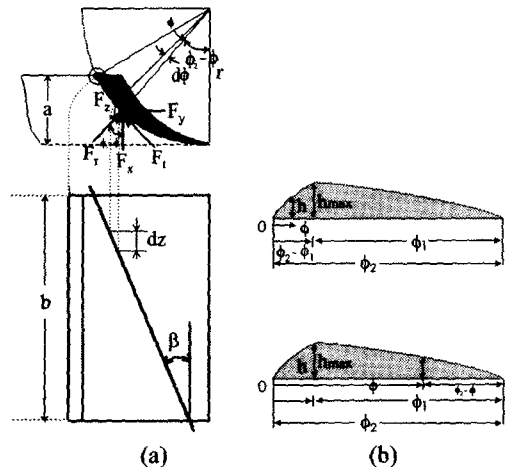Fig. 1 Schematics of down-end milling process

(a) (b)

Fig. 2 (a) Coordinate system for cutting force components and (b) spread undeformed chip cross-sections in down-end milling

The infinitesimal radial and tangential cutting forces (dF_r and dF_t) acting on the tooth are obtained by multiplying the infinitesimal uncut chip area by the specific cutting forces (k_r and k_t) and represented by Eqs. (5) and (6), respectively.

$$dF_r = k_r dA = k_r h dz \qquad (5)$$

$$dF_t = k_t dA = k_t h dz \qquad (6)$$

where dz is the infinitesimal axial depth of cut given by Eq. (7).

$$dz = \frac{r}{\tan \beta} d\phi \qquad (7)$$

To determine the undeformed chip thickness (h), the cross-sectional area of uncut chip shaded in Fig.2 (a) is replaced by the equivalent shaded area with a straight base as shown in Fig. 2 (b).

When ϕ is between the starting point 0 and $\phi_2 - \phi_1$, h can be expressed by Eq. (8).

$$0 \le \phi < \phi_2 - \phi_1$$
$$h = r\left(1 - \frac{\cos \phi_2}{\cos(\phi_2 - \phi)}\right) \qquad (8)$$

If ϕ is between $\phi_2 - \phi_1$ and ϕ_2, h is given as in Eq. (9).

$$\phi_2 - \phi_1 \le \phi < \phi_2 \qquad (9)$$
$$h = s_t r \sin(\phi_2 - \phi)$$

Fig. 3 shows the replaced cross-section of the uncut chip with a straight base and 5 intervals in which positions of the edge are distinguished from one another.
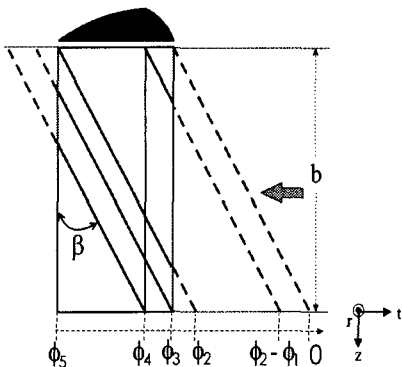

Fig. 3 Cutting edge positions with the rotation angle of the tool

That is necessary for the estimation of cutting forces with the phase change of the tool. The cutting edge is a straight line inclined by β and it moves from right to left. ϕ_3, ϕ_4, and ϕ_5 are as in Eq. (10).

$$\phi_3 = \frac{b\tan\beta}{r}, \qquad \phi_4 = \phi_3 + \phi_2 - \phi_1, \qquad \phi_5 = \phi_3 + \phi_2 \qquad (10)$$

Substituting dz and h of Eqs. (7), (8), and (9) into Eqs. (5) and (6), and combining with Eq. (4), the cutting forces in each interval can be obtained as follows:

$[0, \ \phi_2 - \phi_1]$ interval

$$F_x = \int_0^\phi (k_r \cos(\phi_2 - \phi) + k_t \sin(\phi_2 - \phi)) r\left(1 - \frac{\cos\phi_2}{\cos(\phi_2 - \phi)}\right)\frac{r}{\tan\beta}d\phi$$

$$F_y = \int_0^\phi (-k_r \sin(\phi_2 - \phi) + k_t \cos(\phi_2 - \phi)) r\left(1 - \frac{\cos\phi_2}{\cos(\phi_2 - \phi)}\right)\frac{r}{\tan\beta}d\phi \qquad (11-1)$$

$[\phi_2 - \phi_1, \ \phi_2]$ interval

$$F_x = \int_{\phi_2-\phi_1}^{\phi} (k_r \cos(\phi_2 - \phi) + k_t \sin(\phi_2 - \phi)) s_t \sin(\phi_2 - \phi)\frac{r}{\tan\beta}d\phi +$$
$$\int_0^{\phi_2-\phi_1} (k_r \cos(\phi_2 - \phi) + k_t \sin(\phi_2 - \phi)) r\left(1 - \frac{\cos\phi_2}{\cos(\phi_2 - \phi)}\right)\frac{r}{\tan\beta}d\phi$$

$$F_y = \int_{\phi_2-\phi_1}^{\phi} (-k_r \sin(\phi_2 - \phi) + k_t \cos(\phi_2 - \phi)) s_t \sin(\phi_2 - \phi)\frac{r}{\tan\beta}d\phi +$$
$$\int_0^{\phi_2-\phi_1} (-k_r \sin(\phi_2 - \phi) + k_t \cos(\phi_2 - \phi)) r\left(1 - \frac{\cos\phi_2}{\cos(\phi_2 - \phi)}\right)\frac{r}{\tan\beta}d\phi \qquad (11-2)$$

$[\phi_2, \ \phi_3]$ interval

$$F_x = \int_{\phi_2-\phi_1}^{\phi_2} (k_r \cos(\phi_2 - \phi) + k_t \sin(\phi_2 - \phi)) s_t \sin(\phi_2 - \phi_1)\frac{r}{\tan\beta}d\phi +$$
$$\int_0^{\phi_2-\phi_1} (k_r \cos(\phi_2 - \phi) + k_t \sin(\phi_2 - \phi)) r\left(1 - \frac{\cos\phi_2}{\cos(\phi_2 - \phi)}\right)\frac{r}{\tan\beta}d\phi$$

$$F_y = \int_{\phi_2-\phi_1}^{\phi_2} (-k_r \sin(\phi_2 - \phi) + k_t \cos(\phi_2 - \phi)) s_t \sin(\phi_2 - \phi)\frac{r}{\tan\beta}d\phi +$$
$$\int_0^{\phi_2-\phi_1} (-k_r \sin(\phi_2 - \phi) + k_t \cos(\phi_2 - \phi)) r\left(1 - \frac{\cos\phi_2}{\cos(\phi_2 - \phi)}\right)\frac{r}{\tan\beta}d\phi \qquad (11-3)$$

$[\phi_3, \ \phi_4]$ interval

$$F_x = \int_{\phi_2-\phi_1}^{\phi_2} (k_r \cos(\phi_2 - \phi) + k_t \sin(\phi_2 - \phi)) s_t \sin(\phi_2 - \phi)\frac{r}{\tan\beta}d\phi +$$
$$\int_{\phi-\phi_3}^{\phi_2-\phi_1} (k_r \cos(\phi_2 - \phi) + k_t \sin(\phi_2 - \phi)) r\left(1 - \frac{\cos\phi_2}{\cos(\phi_2 - \phi)}\right)\frac{r}{\tan\beta}d\phi$$

$$F_y = \int_{\phi_2-\phi_1}^{\phi_2} (-k_r \sin(\phi_2 - \phi) + k_t \cos(\phi_2 - \phi)) s_t \sin(\phi_2 - \phi)\frac{r}{\tan\beta}d\phi +$$
$$\int_{\phi-\phi_3}^{\phi_2-\phi_1} (-k_r \sin(\phi_2 - \phi) + k_t \cos(\phi_2 - \phi)) r\left(1 - \frac{\cos\phi_2}{\cos(\phi_2 - \phi)}\right)\frac{r}{\tan\beta}d\phi \qquad (11-4)$$

$[\phi_4, \ \phi_5]$ interval

$$F_x = \int_{\phi-\phi_3}^{\phi_2} (k_r \cos(\phi_2 - \phi) + k_t \sin(\phi_2 - \phi)) s_t \sin(\phi_2 - \phi)\frac{r}{\tan\beta}d\phi$$

$$F_y = \int_{\phi-\phi_3}^{\phi_2} (-k_r \sin(\phi_2 - \phi) + k_t \cos(\phi_2 - \phi)) s_t \sin(\phi_2 - \phi)\frac{r}{\tan\beta}d\phi \qquad (11-5)$$

2.3 Identification of down-end milling with the equivalent oblique cutting system

To establish an equivalent oblique cutting system that is equivalent to an end milling process, cutting and tool geometrical variables must be matched. Oblique cutting is the simplest type of three dimensional cutting achieved by a straight cutting edge that is inclined with respect to the coordinate axis perpendicular to the cutting velocity vector. Fig. 4 shows the unfolded undeformed chips along the workpiece movement direction in a down-end milling process.

In the model of spread end milling, the cutting edges meet the z axis with a helix angle (β), which corresponds to the inclination angle (i) in the equivalent oblique cutting. In addition, the radial rake angle (α_r) in end milling equals the velocity rake angle (α_v) in oblique cutting.
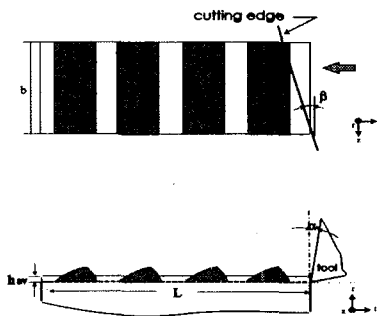

Fig. 4 Spread down-end milling

The average undeformed chip thickness, h_{av}, is determined on the basis of the same volume of chip produced in end milling and the equivalent oblique cutting process as given in Eq. (12).

$$h_{av} = \frac{a\ S_t\ Z}{\pi\ d} \qquad (12)$$

where d is the tool diameter, Z is the number of tooth, S_t is the feed per tooth, and a is the radial depth of cut in end milling.

The axial depth of cut (b) and cutting velocity (V) in end milling are equal to the width of cut (b) and cutting velocity (V) in the equivalent oblique cutting, respectively. Accordingly, the spread end milling process can be reduced to an equivalent continuous oblique cutting process with a constant undeformed chip thickness.

3. Cutting experiments

Two sets of experiments were performed to verify the proposed force model. End-mills of 8mm diameter with 20° helix angles were used in the end milling tests. Table 1 shows the cutting test conditions of the down-end milling and the equivalent oblique cutting. To identify the cutting conditions of the two processes, the undeformed chip thickness in the oblique cutting is determined using Eq. (12). The three cutting force components were measured using a piezo-type tool dynamometer and force signals were digitized and stored using a micro-processor-controlled data acquisition system (Fig.5).
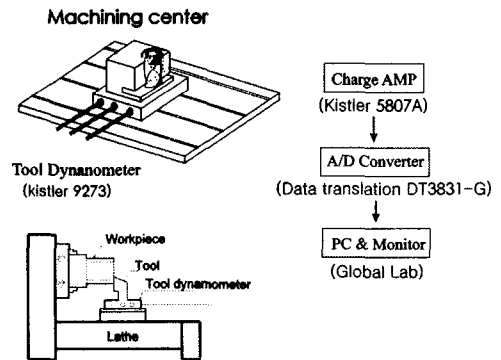

Fig.5 Schematic diagram for experimental setup

Table 1 Cutting conditions

Down end milling	
Work material	SM45C
Radial depth of cut, a (mm)	3
Axial depth of cut, b (mm)	2
Cutting velocity, V (m/min)	15.9
Radial rake angle, α_r (deg.)	6
Helix angle, β(deg.)	20
Number of teeth, Z	2
Feed per tooth, S_t (mm) 0.2051,0.2303,0.2428,0.2554,0.2805	
Equivalent Oblique cutting	
Work material	SM45C
Width of cut, b (mm)	2
Cutting velocity, V (m/min)	15.9
Velocity rake angle, α_v (deg.)	6
Inclination angle, i (deg.)	20
undeformed chip thickness, t (mm/rev) 0.049,0.055,0.058,0.061,0.067	

4. Results and discussions

To obtain reliable radial and tangential cutting forces at a given instant, the measured cutting force components and the undeformed chip areas should be matched precisely to that moment. To meet this condition, as a first step, the specific cutting forces are calculated assuming that the measured cutting force is matched with the undeformed chip area at a given instant. Then, the values of the next instant are to be calculated with an area which is adjacent to the first with a suitable interval.

Since each data is obtained with 1.85° interval of the tool rotation angle, 44 data groups are obtained during cutting of one tooth. Selecting the group which shows the lowest standard deviation of the specific cutting forces, k_r and k_t, among the 44 data groups as seen in Fig. 6, it can be found that the cutting force component variations coincide well with those of the undeformed chip area.
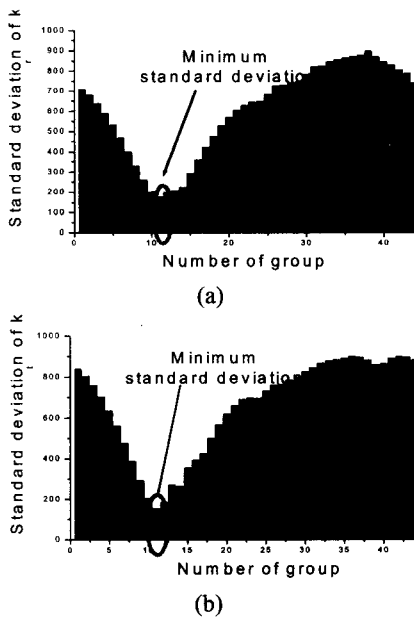

(a)

(b)

Fig. 6 Standard deviation of (a) k_r and (b) k_t in down- end milling (0.2051 mm/tooth)

4.1 Cutting force and chip thickness

Substituting the measured cutting force components, F_x and F_y, for Eq. (11), the specific cutting forces, k_r and k_t, can be obtained. The tangential (F_t) and radial (F_r) cutting forces are estimated by multiplying the undeformed cut area by the specific cutting forces. The main (F_y), the feed (F_z), and the thrust (F_x) cutting forces

in the equivalent oblique cutting model correspond to the tangential (F_t), the radial (F_r), and the axial (F_z) cutting forces in the end milling, respectively.

Fig. 7 shows the measured forces (F_x, F_y), and the tangential and radial forces (F_r, F_t), with the lowest (0.2051mm/tooth) and largest (0.2805mm /tooth) feed per tooth among the given conditions. Fig. 8 shows the cutting forces of the equivalent oblique cutting model to the down-end milling process and the oblique cutting tests along with the equivalent undeformed chip thickness. The cutting forces in down-end milling and oblique cutting tests increase as the equivalent undeformed chip thickness increases as shown in the figure. There is no significant difference between the two sets of cutting forces.
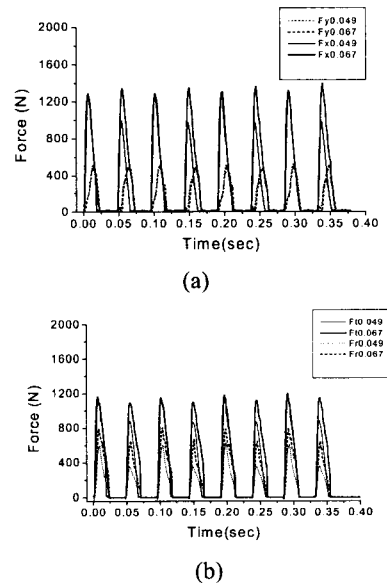

(a)

(b)

Fig. 7 (a) Measured forces (F_x, F_y) and (b) tangential and radial forces (F_t, F_r) in down-end milling
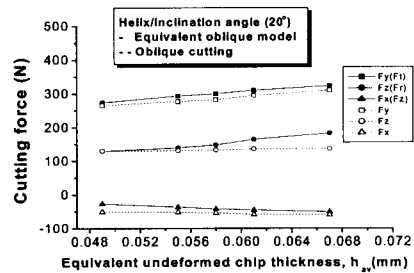

Fig. 8 Cutting forces in equivalent oblique model to down-end milling and oblique cutting test

23

The measured chip thicknesses are given in Table 2. The values of feed per tooth in the table match with those of the undeformed chip thickness of the oblique cutting. As seen in the table, the chip thickness of the oblique cutting is slightly lager than that of end milling except for the condition of 0.2051 mm/tooth.

Table 2 Chip thickness

Down end milling		Oblique cutting	
Feed per tooth, S_t (mm)	Averaged chip thickness (mm)	Undeformed chip thickness, h_{av}(mm)	Chip thickness (mm)
0.2051	0.113	0.049	0.107
0.2303	0.122	0.055	0.124
0.2428	0.129	0.058	0.132
0.2554	0.139	0.061	0.140
0.2805	0.144	0.067	0.150

4.2 Shear and friction characteristics

Table 3 shows the friction and shear characteristic factors in the down-end milling and oblique cutting processes. The factors can be calculated by substituting the replaced cutting forces into the oblique cutting model.[7]

The friction forces and the specific friction energy consumed in end milling process are somewhat larger than those of the oblique cutting. While the shear forces and specific shear energy were vice versa. 68~75% and 70~71% of the total energy is consumed in the shear processes in down-end milling and oblique cutting processes, respectively. The specific cutting energy decreases with increase of undeformed thickness in the end milling process. These results coincide well with the results of the continuous cutting process.[7,8]

Table 3 Shear and friction characteristics

Helix/inclination angle (20°)		
	Down end milling	Oblique cutting
Friction Characteristics		
Friction force, F_c (N)	155.7~221.8	161.8~173.8
Specific friction energy, u (Mpa)	685.22~768.5	783.3~682.1
Shear Characteristics		
Shear force, F_s (N)	207.5~221.2	189.9~230.8
Specific shear energy, u_s (Mpa)	2108.8~1639.9	1957.7~1736.8
Cutting Characteristics		
Specific cutting energy, u (Mpa)	2794.0~2408.5	2711.8~2315.1
u_f/u	0.23~0.31	0.29~0.30
u_s/u	0.75 ~ 0.68	0.71 ~ 0.70

5. Conclusions

The equivalent oblique cutting model has been proposed to analyze the friction and shear characteristics of a down-end milling process. The model was verified through two sets of experiments. The experimental results show that:

1) The proposed model is suitable to analyze the shear and chip-tool frictional characteristics in a down-end milling process.

2) There is no significant difference between the two sets of cutting forces and chip thicknesses in end milling and oblique cutting processes.

3) The specific cutting energy decreases with increase in the equivalent undeformed thickness in down-end milling and oblique cutting processes.

References

1. Martellotti, M. E., "An Analysis of the Milling Process," Trans. ASME, Vol. 63, pp. 677-700, 1941.

2. Tlusty, J. and Macneil, P., "Dynamics of Cutting Forces in End Milling," Annals of CIRP, Vol. 24, pp. 21-25, 1975.

3. Zheng, L., Liang, S. Y. and Melkote, S. N., "Angle Domain Analytical Model for End Milling Forces," ASME, J. Man. Sci. and Eng., Vol. 120, pp. 252-258, 1998.

4. Yang, M. Y. and Choi, J. G., "A Tool Deflection Compensation System for End Milling Accuracy Improvement," ASME, J. Man. Sci. and Eng., Vol. 120, pp. 222-229, 1998.

5. Altintas, Y., Engin, S. and Budak, E., "Analytical Stability Prediction and Design of Variable Pitch Cutters," ASME, J. Man. Sci. and Eng., Vol. 121, pp. 173-178, 1999.

6. Lee, Y. M., Yang, S. H. and Jang, S. I., "Shear and friction process in intermittent cutting," IJMPB, Vol. 17, Nos. 8 & 9, pp. 1395-1400, 2003.

7. Lee, Y. M., Choi, W. S. and Song, T. S., "Analysis of 3-D Cutting Process with Single Point Tool," J. of the KSPE, Vol. 1, No. 1, pp. 15-21, 2000.

8. Shaw, M. C., Cook, N. H. and Smith, P. A., "The Mechanics of Three dimensional Cutting Operations," Trans. ASME, Vol. 73, pp. 1055-1064, 1951.